

# Supplementary Material

## Adversarially Robust Optimization with Gaussian Processes

Ilija Bogunovic, Jonathan Scarlett, Stefanie Jegelka and Volkan Cevher (NeurIPS 2018)

### A Illustration of STABLEOPT's Execution

The following figure gives an example of the selection procedure of STABLEOPT at two different time steps:

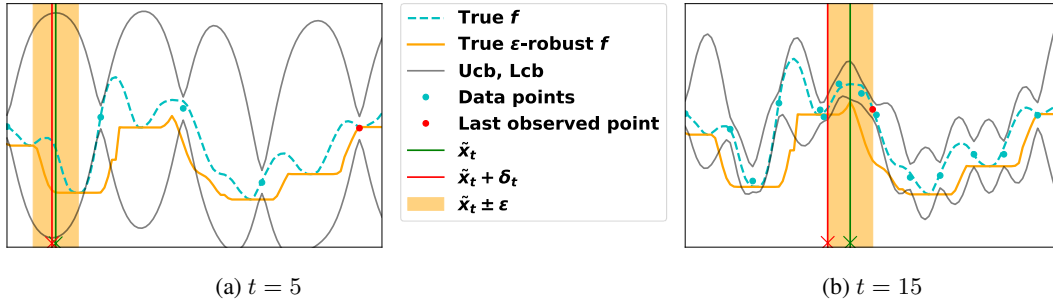
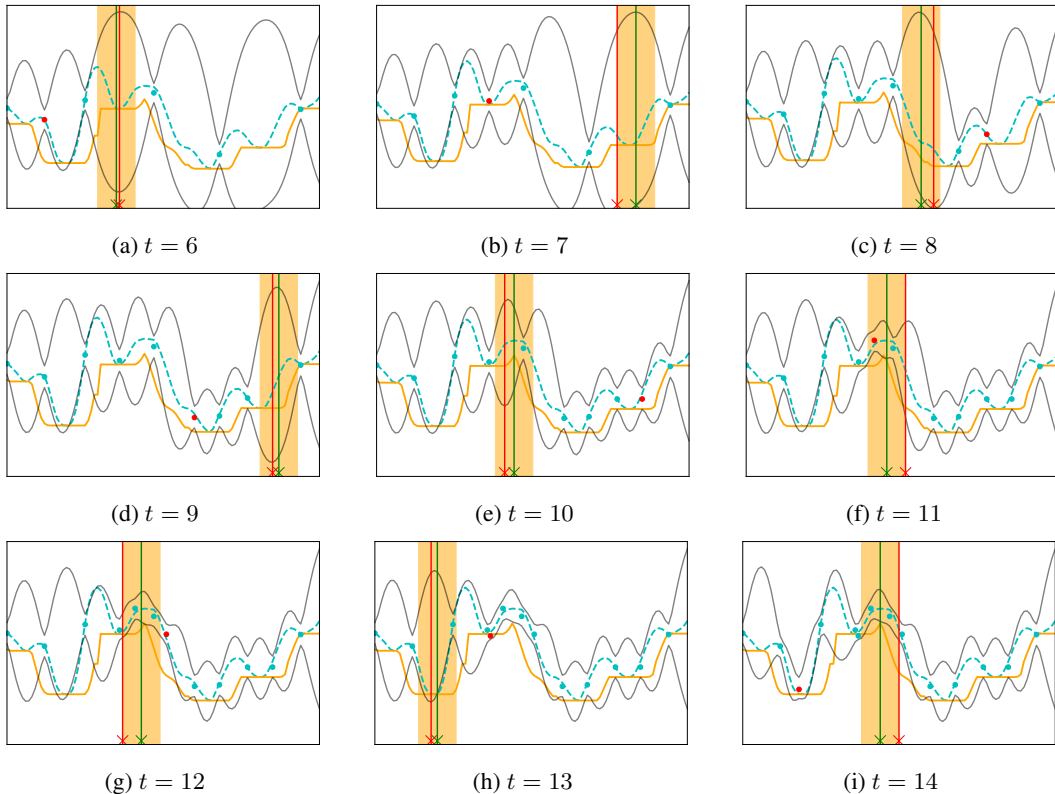


Figure 4: An execution of STABLEOPT on the running example. We observe that after  $t = 15$  steps,  $\tilde{x}_t$  obtained in Eq. 13 corresponds to  $x_\epsilon^*$ .

The intermediate time steps are illustrated as follows:



## B Proofs of Theoretical Results

### B.1 Proof of Theorem 1 (upper bound)

Recall that  $\tilde{\mathbf{x}}_t$  is the point computed by STABLEOPT in (13) at time  $t$ , and that  $\boldsymbol{\delta}_t$  corresponds to the perturbation obtained in STABLEOPT (Line 3) at time  $t$ . In the following, we condition on the event in Lemma 1 holding true, meaning that  $\text{ucb}_t$  and  $\text{lcb}_t$  provide valid confidence bounds as per (15). As stated in the lemma, this holds with probability at least  $1 - \xi$ .

By the definition of  $\epsilon$ -instant regret, we have

$$r_\epsilon(\tilde{\mathbf{x}}_t) = \max_{\mathbf{x} \in D} \min_{\boldsymbol{\delta} \in \Delta_\epsilon(\mathbf{x})} f(\mathbf{x} + \boldsymbol{\delta}) - \min_{\boldsymbol{\delta} \in \Delta_\epsilon(\tilde{\mathbf{x}}_t)} f(\tilde{\mathbf{x}}_t + \boldsymbol{\delta}) \quad (32)$$

$$\leq \max_{\mathbf{x} \in D} \min_{\boldsymbol{\delta} \in \Delta_\epsilon(\mathbf{x})} f(\mathbf{x} + \boldsymbol{\delta}) - \min_{\boldsymbol{\delta} \in \Delta_\epsilon(\tilde{\mathbf{x}}_t)} \text{lcb}_{t-1}(\tilde{\mathbf{x}}_t + \boldsymbol{\delta}) \quad (33)$$

$$= \max_{\mathbf{x} \in D} \min_{\boldsymbol{\delta} \in \Delta_\epsilon(\mathbf{x})} f(\mathbf{x} + \boldsymbol{\delta}) - \text{lcb}_{t-1}(\tilde{\mathbf{x}}_t + \boldsymbol{\delta}_t) \quad (34)$$

$$\leq \max_{\mathbf{x} \in D} \min_{\boldsymbol{\delta} \in \Delta_\epsilon(\mathbf{x})} \text{ucb}_{t-1}(\mathbf{x} + \boldsymbol{\delta}) - \text{lcb}_{t-1}(\tilde{\mathbf{x}}_t + \boldsymbol{\delta}_t) \quad (35)$$

$$= \min_{\boldsymbol{\delta} \in \Delta_\epsilon(\tilde{\mathbf{x}}_t)} \text{ucb}_{t-1}(\tilde{\mathbf{x}}_t + \boldsymbol{\delta}) - \text{lcb}_{t-1}(\tilde{\mathbf{x}}_t + \boldsymbol{\delta}_t) \quad (36)$$

$$\leq \text{ucb}_{t-1}(\tilde{\mathbf{x}}_t + \boldsymbol{\delta}_t) - \text{lcb}_{t-1}(\tilde{\mathbf{x}}_t + \boldsymbol{\delta}_t) \quad (37)$$

$$= 2\beta_t^{1/2} \sigma_{t-1}(\tilde{\mathbf{x}}_t + \boldsymbol{\delta}_t), \quad (38)$$

where (33) and (35) follow from Lemma 1, (34) follows since  $\boldsymbol{\delta}_t$  minimizes  $\text{lcb}_{t-1}$  by definition, (36) follows since  $\tilde{\mathbf{x}}_t$  maximizes the robust upper confidence bound by definition, (37) follows by upper bounding the minimum by the specific choice  $\boldsymbol{\delta}_t \in \Delta_\epsilon(\tilde{\mathbf{x}}_t)$ , and (38) follows since the upper and lower confidence bounds are separated by  $2\beta_t^{1/2} \sigma_{t-1}(\cdot)$  according to their definitions in (12).

In fact, the analysis from (33) to (38) shows that the following *pessimistic estimate* of  $r_\epsilon(\tilde{\mathbf{x}}_t)$  is upper bounded by  $2\beta_t^{1/2} \sigma_{t-1}(\tilde{\mathbf{x}}_t + \boldsymbol{\delta}_t)$ :

$$\bar{r}_\epsilon(\tilde{\mathbf{x}}_t) = \max_{\mathbf{x} \in D} \min_{\boldsymbol{\delta} \in \Delta_\epsilon(\mathbf{x})} f(\mathbf{x} + \boldsymbol{\delta}) - \min_{\boldsymbol{\delta} \in \Delta_\epsilon(\tilde{\mathbf{x}}_t)} \text{lcb}_{t-1}(\tilde{\mathbf{x}}_t + \boldsymbol{\delta}). \quad (39)$$

Unlike  $r_\epsilon(\tilde{\mathbf{x}}_t)$ , the algorithm has the required knowledge to identify the value of  $t \in \{1, \dots, T\}$  with the smallest  $\bar{r}_\epsilon(\tilde{\mathbf{x}}_t)$ . Specifically, the first term on the right-hand side of (39) does not depend on  $t$ , so the smallest  $\bar{r}_\epsilon(\tilde{\mathbf{x}}_t)$  is achieved by  $\mathbf{x}^{(T)}$  defined in (17). Since the minimum is upper bounded by the average, it follows that

$$r_\epsilon(\mathbf{x}^{(T)}) \leq \bar{r}_\epsilon(\mathbf{x}^{(T)}) \quad (40)$$

$$\leq \frac{1}{T} \sum_{t=1}^T 2\beta_t^{1/2} \sigma_{t-1}(\tilde{\mathbf{x}}_t + \boldsymbol{\delta}_t) \quad (41)$$

$$\leq \frac{2\beta_T^{1/2}}{T} \sum_{t=1}^T \sigma_{t-1}(\tilde{\mathbf{x}}_t + \boldsymbol{\delta}_t), \quad (42)$$

where (41) uses (38), and (42) uses the monotonicity of  $\beta_T$ . Next, we claim that

$$2 \sum_{t=1}^T \sigma_{t-1}(\tilde{\mathbf{x}}_t + \boldsymbol{\delta}_t) \leq \sqrt{C_1 T \gamma_T}, \quad (43)$$

where  $C_1 = 8/\log(1 + \sigma^{-2})$ . In fact, this is a special case of the well-known result [31, Lemma 5.4]<sup>4</sup> which upper bounds the sum of posterior standard deviations of sampled points in terms of the information gain  $\gamma_T$  (recall that STABLEOPT samples at location  $\tilde{\mathbf{x}}_t + \boldsymbol{\delta}_t$ ). Combining (42)–(43) and re-arranging, we deduce that after  $T$  satisfies  $\frac{T}{\beta_T \gamma_T} \geq \frac{C_1}{\eta^2}$ , the  $\epsilon$ -instant regret is at most  $\eta$ , thus completing the proof.

<sup>4</sup>More precisely, [31, Lemma 5.4] alongside an application of the Cauchy-Schwarz inequality as in [31].

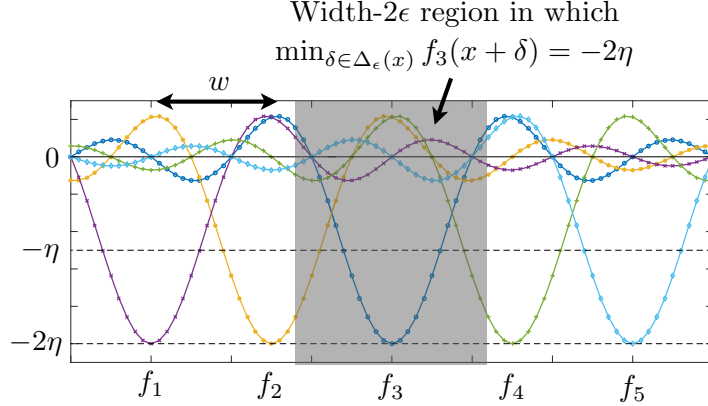


Figure 6: Illustration of functions  $f_1, \dots, f_5$  equal to a common function shifted by various multiples of a given parameter  $w$ . In the  $\epsilon$ -stable setting, there is a wide region (shown in gray for the dark blue curve  $f_3$ ) within which the perturbed function value equals  $-2\eta$ .

## B.2 Proof of Theorem 2 (lower bound)

Our lower bounding analysis builds heavily on that of the non-robust optimization setting with  $f \in \mathcal{F}_k(B)$  studied in [27], but with important differences. Roughly speaking, the analysis of [27] is based on the difficulty of finding a very narrow “bump” of height  $2\eta$  in a function whose values are mostly close to zero. In the  $\epsilon$ -stable setting, however, even the points around such a bump will be adversarially perturbed to another point whose function value is nearly zero. Hence, all points are essentially equally bad.

To overcome this challenge, we consider the reverse scenario: Most of the function values are still nearly zero, but there exists a narrow *valley* of depth  $-2\eta$ . This means that every point within an  $\epsilon$ -ball around the function minimizer will be perturbed to the point with value  $-2\eta$ . Hence, a constant fraction of the volume is still  $2\eta$ -suboptimal, and it is impossible to avoid this region with high probability unless the time horizon  $T$  is sufficiently large. An illustration is given in Figure 6, with further details below.

We now proceed with the formal proof.

### B.2.1 Preliminaries

Recall that we are considering an arbitrary given (deterministic) GP optimization algorithm. More precisely, such an algorithm consists of a sequence of decision functions that return a sampling location  $\mathbf{x}_t$  based on  $y_1, \dots, y_{t-1}$ , and an additional decision function that reports the final point  $\mathbf{x}^{(T)}$  based on  $y_1, \dots, y_T$ . The points  $\mathbf{x}_1, \dots, \mathbf{x}_{t-1}$  (or  $\mathbf{x}_1, \dots, \mathbf{x}_T$ ) do not need to be treated as additional inputs to these functions, since  $(\mathbf{x}_1, \dots, \mathbf{x}_{t-1})$  is a deterministic function of  $(y_1, \dots, y_{t-1})$ .

We first review several useful results and techniques from [27]:

- We lower bound the worst-case  $\epsilon$ -regret within  $\mathcal{F}_k(B)$  by the  $\epsilon$ -regret averaged over a suitably-designed finite collection  $\{f_1, \dots, f_M\} \subset \mathcal{F}_k(B)$  of size  $M$ .
- We choose each  $f_m(\mathbf{x})$  to be a shifted version of a common function  $g(\mathbf{x})$  on  $\mathbb{R}^p$ . Specifically, each  $f_m(\mathbf{x})$  is obtained by shifting  $g(\mathbf{x})$  by a different amount, and then cropping to  $D = [0, 1]^p$ . For our purposes, we require  $g(\mathbf{x})$  to satisfy the following properties:
  1. The RKHS norm in  $\mathbb{R}^p$  is bounded,  $\|g\|_k \leq B$ ;
  2. We have (i)  $g(\mathbf{x}) \in [-2\eta, 2\eta]$  with minimum value  $g(0) = -2\eta$ , and (ii) there is a “width”  $w$  such that  $g(\mathbf{x}) > -\eta$  for all  $\|\mathbf{x}\|_\infty \geq w$ ;
  3. There are absolute constants  $h_0 > 0$  and  $\zeta > 0$  such that  $g(\mathbf{x}) = \frac{2\eta}{h_0} h\left(\frac{\mathbf{x}\zeta}{w}\right)$  for some function  $h(\mathbf{z})$  that decays faster than any finite power of  $\|\mathbf{z}\|_2^{-1}$  as  $\|\mathbf{z}\|_2 \rightarrow \infty$ .

Letting  $g(\mathbf{x})$  be such a function, we construct the  $M$  functions by shifting  $g(\mathbf{x})$  so that each  $f_m(\mathbf{x})$  is centered on a unique point in a uniform grid, with points separated by  $w$  in each dimension. Since  $D = [0, 1]^p$ , one can construct

$$M = \left\lfloor \left( \frac{1}{w} \right)^p \right\rfloor \quad (44)$$

such functions. We will use this construction with  $w \ll 1$ , so that there is no risk of having  $M = 0$ , and in fact  $M$  can be assumed larger than any desired absolute constant.

- It is shown in [27] that the above properties<sup>5</sup> can be achieved with

$$M = \left\lfloor \left( \frac{r \sqrt{\log \frac{B(2\pi l^2)^{p/4} h(0)}{2\eta}}}{\zeta \pi l} \right)^p \right\rfloor \quad (45)$$

in the case of the SE kernel, and with

$$M = \left\lfloor \left( \frac{Bc_3}{\eta} \right)^{p/\nu} \right\rfloor \quad (46)$$

in the case of the Matérn kernel, where

$$c_3 := \left( \frac{r}{\zeta} \right)^\nu \cdot \left( \frac{c_2^{-1/2}}{2(8\pi^2)^{(\nu+p/2)/2}} \right), \quad (47)$$

and where  $c_2 > 0$  is an absolute constant. Note that these values of  $M$  amount to choosing  $w$  in (44), and the assumption of sufficiently small  $\frac{\eta}{B}$  in the theorem statement ensures that  $M \gg 1$  (or equivalently  $w \ll 1$ ) as stated above.

- Property 2 above ensures that the “robust” function value  $\min_{\delta \in \Delta_\epsilon(\mathbf{x})} f(\mathbf{x})$  equals  $-2\eta$  for any  $\mathbf{x}$  whose  $\epsilon$ -neighborhood includes the minimizer  $\mathbf{x}_{\min}$  of  $f$ , while being  $-\eta$  or higher for any input whose entire  $\epsilon$ -neighborhood is separated from  $\mathbf{x}_{\min}$  by at least  $w$ . For  $w \ll 1$  and  $\epsilon < 0.5$ , a point of the latter type is guaranteed to exist, which implies

$$r_\epsilon(\mathbf{x}) \geq \eta \quad (48)$$

for any  $\mathbf{x}$  whose  $\epsilon$ -neighborhood includes  $\mathbf{x}_{\min}$ .

In addition, we introduce the following notation, also used in [27]:

- The probability density function of the output sequence  $\mathbf{y} = (y_1, \dots, y_T)$  when the underlying function is  $f_m$  is denoted by  $P_m(\mathbf{y})$ . We also define  $f_0(\mathbf{x}) = 0$  to be the zero function, and define  $P_0(\mathbf{y})$  analogously for the case that the optimization algorithm is run on  $f_0$ . Expectations and probabilities (with respect to the noisy observations) are similarly written as  $\mathbb{E}_m, \mathbb{P}_m, \mathbb{E}_0,$  and  $\mathbb{P}_0$  when the underlying function is  $f_m$  or  $f_0$ . On the other hand, in the absence of a subscript,  $\mathbb{E}[\cdot]$  and  $\mathbb{P}[\cdot]$  are taken with respect to the noisy observations *and* the random function  $f$  drawn uniformly from  $\{f_1, \dots, f_M\}$  (recall that we are lower bounding the worst case by this average).
- Let  $\{\mathcal{R}_m\}_{m=1}^M$  be a partition of the domain into  $M$  regions according the above-mentioned uniform grid, with  $f_m$  taking its minimum value of  $-2\eta$  in the centre of  $\mathcal{R}_m$ . Moreover, let  $j_t$  be the index at time  $t$  such that  $\mathbf{x}_t$  falls into  $\mathcal{R}_{j_t}$ ; this can be thought of as a quantization of  $\mathbf{x}_t$ .
- Define the maximum (absolute) function value within a given region  $\mathcal{R}_j$  as

$$\bar{v}_m^j := \max_{\mathbf{x} \in \mathcal{R}_j} |f_m(\mathbf{x})|, \quad (49)$$

and the maximum KL divergence to  $P_0$  within the region as

$$\bar{D}_m^j := \max_{\mathbf{x} \in \mathcal{R}_j} D(P_0(\cdot|\mathbf{x}) \| P_m(\cdot|\mathbf{x})), \quad (50)$$

where  $P_m(y|\mathbf{x})$  is the distribution of an observation  $y$  for a given selected point  $\mathbf{x}$  under the function  $f_m$ , and similarly for  $P_0(y|\mathbf{x})$ .

<sup>5</sup>Here  $g(\mathbf{x})$  plays the role of  $-g(\mathbf{x})$  in [27] due to the discussion at the start of this appendix, but otherwise the construction is identical.

- Let  $N_j \in \{0, \dots, T\}$  be a random variable representing the number of points from  $\mathcal{R}_j$  that are selected throughout the  $T$  rounds.

Next, we present several useful lemmas. The following well-known change-of-measure result, which can be viewed as a form of Le Cam’s method, has been used extensively in both discrete and continuous bandit problems.

**Lemma 2.** [1, p. 27] *For any function  $a(\mathbf{y})$  taking values in a bounded range  $[0, A]$ , we have*

$$|\mathbb{E}_m[a(\mathbf{y})] - \mathbb{E}_0[a(\mathbf{y})]| \leq A d_{\text{TV}}(P_0, P_m) \quad (51)$$

$$\leq A \sqrt{D(P_0 \| P_m)}, \quad (52)$$

where  $d_{\text{TV}}(P_0, P_m) = \frac{1}{2} \int_{\mathbb{R}^T} |P_0(\mathbf{y}) - P_m(\mathbf{y})| d\mathbf{y}$  is the total variation distance.

We briefly remark on some slight differences here compared to [1, p. 27]. There, only  $\mathbb{E}_m[a(\mathbf{y})] - \mathbb{E}_0[a(\mathbf{y})]$  is upper bounded in terms of  $d_{\text{TV}}(P_0, P_m)$ , but one easily obtains the same upper bound on  $\mathbb{E}_0[a(\mathbf{y})] - \mathbb{E}_m[a(\mathbf{y})]$  by interchanging the roles of  $P_0$  and  $P_m$ . The step (52) follows from Pinsker’s inequality,  $d_{\text{TV}}(P_0, P_m) \leq \sqrt{\frac{D(P_0 \| P_m)}{2}}$ , and by upper bounding  $\frac{1}{\sqrt{2}} \leq 1$  to ease the notation.

The following result simplifies the divergence term in (52).

**Lemma 3.** [27, Eq. (44)] *Under the preceding definitions, we have*

$$D(P_0 \| P_m) \leq \sum_{j=1}^M \mathbb{E}_0[N_j] \bar{D}_m^j. \quad (53)$$

The following well-known property gives a formula for the KL divergence between two Gaussians.

**Lemma 4.** [27, Eq. (36)] *For  $P_1$  and  $P_2$  being Gaussian with means  $(\mu_1, \mu_2)$  and a common variance  $\sigma^2$ , we have*

$$D(P_1 \| P_2) = \frac{(\mu_1 - \mu_2)^2}{2\sigma^2}. \quad (54)$$

Finally, we have the following technical result regarding the “needle-in-haystack” type function constructed above.

**Lemma 5.** [27, Lemma 7] *The functions  $\{f_m\}_{m=1}^M$  corresponding to (45)–(46) are such that the quantities  $\bar{v}_m^j$  satisfy  $\sum_{m=1}^M (\bar{v}_m^j)^2 = O(\eta^2)$  for all  $j$ .*

## B.2.2 Analysis of the average $\epsilon$ -stable regret

Let  $J_{\text{bad}}(m)$  be the set of  $j$  such that all  $\mathbf{x} \in \mathcal{R}_j$  yield  $\min_{\boldsymbol{\delta} \in \Delta_\epsilon(\mathbf{x})} f(\mathbf{x} + \boldsymbol{\delta}) = -2\eta$  when the true function is  $f_m$ , and define  $\mathcal{R}_{\text{bad}}(m) = \cup_{j \in J_{\text{bad}}(m)} \mathcal{R}_j$ . By the  $\epsilon$ -regret lower bound in (48), we have

$$\mathbb{E}_m[r_\epsilon(\mathbf{x}^{(T)})] \geq \eta \mathbb{P}_m[\mathbf{x}^{(T)} \in \mathcal{R}_{\text{bad}}(m)] \quad (55)$$

$$\geq \eta \left( \mathbb{P}_0[\mathbf{x}^{(T)} \in \mathcal{R}_{\text{bad}}(m)] - \sqrt{D(P_0 \| P_m)} \right) \quad (56)$$

$$\geq \eta \left( \mathbb{P}_0[\mathbf{x}^{(T)} \in \mathcal{R}_{\text{bad}}(m)] - \sqrt{\sum_{j=1}^M \mathbb{E}_0[N_j] \bar{D}_m^j} \right), \quad (57)$$

where (56) follows from Lemma 2 with  $a(\mathbf{y}) = \mathbf{1}\{\mathbf{x}^{(T)} \in \mathcal{R}_{\text{bad}}(m)\}$  and  $A = 1$  (recall that  $\mathbf{x}^{(T)}$  is a function of  $\mathbf{y} = (y_1, \dots, y_T)$ ), and (57) follows from Lemma 3. Averaging over  $m$  uniform on  $\{1, \dots, M\}$ , we obtain

$$\mathbb{E}[r_\epsilon(\mathbf{x}^{(T)})] \geq \eta \left( \frac{1}{M} \sum_{m=1}^M \mathbb{P}_0[\mathbf{x}^{(T)} \in \mathcal{R}_{\text{bad}}(m)] - \frac{1}{M} \sum_{m=1}^M \sqrt{\sum_{j=1}^M \mathbb{E}_0[N_j] \bar{D}_m^j} \right). \quad (58)$$

We proceed by bounding the two terms separately.

- We first claim that

$$\frac{1}{M} \sum_{m=1}^M \mathbb{P}_0[\mathbf{x}^{(T)} \in \mathcal{R}_{\text{bad}}(m)] \geq C_1 \quad (59)$$

for some  $C_1 > 0$ . To show this, it suffices to prove that any given  $\mathbf{x}^{(T)} \in D$  is in at least a constant fraction of the  $\mathcal{R}_{\text{bad}}(m)$  regions, of which there are  $M$ . This follows from the fact that the  $\epsilon$ -ball centered at  $\mathbf{x}_{m,\min} = \arg \min_{\mathbf{x} \in D} f_m(\mathbf{x})$  takes up a constant fraction of the volume of  $D$ , where the constant depends on both the stability parameter  $\epsilon$  and the dimension  $p$ . A small caveat is that because the definition of  $\mathcal{R}_{\text{bad}}$  insists that the *every* point in the region  $\mathcal{R}_j$  is within distance  $\epsilon$  of  $\mathbf{x}_{m,\min}$ , the left-hand side of (59) may be slightly below the relevant ratio of volumes above. However, since Theorem 2 assumes that  $\frac{\eta}{B}$  is sufficiently small, the choices of  $M$  in (45) and (46) ensure that  $M$  is sufficiently large for this “quantization” effect to be negligible.

- For the second term in (58), we claim that

$$\frac{1}{M} \sum_{m=1}^M \sqrt{\sum_{j=1}^M \mathbb{E}_0[N_j] \bar{D}_m^j} \leq C_2 \frac{\eta}{\sigma} \sqrt{\frac{T}{M}} \quad (60)$$

for some  $C_2 > 0$ . To see this, we write

$$\begin{aligned} & \frac{1}{M} \sum_{m=1}^M \sqrt{\sum_{j=1}^M \mathbb{E}_0[N_j] \bar{D}_m^j} \\ &= O\left(\frac{1}{\sigma}\right) \cdot \frac{1}{M} \sum_{m=1}^M \sqrt{\sum_{j=1}^M \mathbb{E}_0[N_j] (\bar{v}_m^j)^2} \end{aligned} \quad (61)$$

$$\leq O\left(\frac{1}{\sigma}\right) \cdot \sqrt{\frac{1}{M} \sum_{m=1}^M \sum_{j=1}^M \mathbb{E}_0[N_j] (\bar{v}_m^j)^2} \quad (62)$$

$$= O\left(\frac{1}{\sigma}\right) \cdot \sqrt{\frac{1}{M} \sum_{j=1}^M \mathbb{E}_0[N_j] \left(\sum_{m=1}^M (\bar{v}_m^j)^2\right)} \quad (63)$$

$$= O\left(\frac{\eta}{\sqrt{M}\sigma}\right) \cdot \sqrt{\sum_{j=1}^M \mathbb{E}_0[N_j]} \quad (64)$$

$$= O\left(\frac{\sqrt{T}\eta}{\sqrt{M}\sigma}\right), \quad (65)$$

where (61) follows since the divergence  $D(P_0(\cdot|\mathbf{x})\|P_m(\cdot|\mathbf{x}))$  associated with a point  $\mathbf{x}$  having value  $v(\mathbf{x})$  is  $\frac{v(\mathbf{x})^2}{2\sigma^2}$  (cf., (54)), (62) follows from Jensen’s inequality, (64) follows from Lemma 5, and (65) follows from  $\sum_j N_j = T$ .

Substituting (59) and (60) into (58), we obtain

$$\mathbb{E}[r_\epsilon(\mathbf{x}^{(T)})] \geq \eta \left( C_1 - C_2 \frac{\eta}{\sigma} \sqrt{\frac{T}{M}} \right), \quad (66)$$

which implies that the regret is lower bounded by  $\Omega(\eta)$  unless  $T = \Omega\left(\frac{M\sigma^2}{\eta^2}\right)$ . Substituting  $M$  from (45) and (46), we deduce that the conditions on  $T$  in the theorem statement are necessary to achieve average regret  $\mathbb{E}[r_\epsilon(\mathbf{x}^{(T)})] = O(\eta)$  with a sufficiently small implied constant.

### B.2.3 From average to high-probability regret

Recall that we are considering functions whose values lie in the range  $[-2\eta, 2\eta]$ , implying that  $r_\epsilon(\mathbf{x}^{(T)}) \leq 4\eta$ . Letting  $T_\eta$  be the lower bound on  $T$  derived above for achieving average regret

$O(\eta)$  (i.e., we have  $\mathbb{E}[r_\epsilon^{(T_\eta)}] = \Omega(\eta)$ ), it follows from the reverse Markov inequality (i.e., Markov’s inequality applied to the random variable  $4\eta - r_\epsilon^{(T_\eta)}$ ) that

$$\mathbb{P}[r_\epsilon(\mathbf{x}^{(T_\eta)}) \geq c\eta] \geq \frac{\Omega(\eta) - c\eta}{4\eta - c\eta} \quad (67)$$

for any  $c > 0$  sufficiently small for the numerator and denominator to be positive. The right-hand side is lower bounded by a constant for any such  $c$ , implying that the probability of achieving  $\epsilon$ -regret at most  $c\eta$  cannot be arbitrarily close to one. By renaming  $c\eta$  as  $\eta'$ , it follows that in order to achieve some target  $\epsilon$ -stable regret  $\eta'$  with probability sufficiently close to one, a lower bound of the same form as the average regret bound holds. In other words, the conditions on  $T$  in the theorem statement remain necessary also for the high-probability regret.

We emphasize that Theorem 2 concerns the high-probability regret when “high probability” means *sufficiently close to one* as a function of  $\epsilon$ ,  $p$ , and the kernel parameters (but still constant with respect to  $T$  and  $\eta$ ). We do not claim a lower bound under any particular *given* success probability (e.g.,  $\eta$ -optimality with probability at least  $\frac{3}{4}$ ).

## C Details on Variations from Section 4

We claim that the STABLEOPT variations and theoretical results outlined in Section 4 are in fact special cases of Algorithm 1 and Theorem 1, despite being seemingly quite different. The idea behind this claim is that Algorithm 1 and Theorem 1 allow for the “distance” function  $d(\cdot, \cdot)$  to be completely arbitrary, so we may choose it in rather creative/unconventional ways.

In more detail, we have the following:

- For the unknown parameter setting  $\max_{\mathbf{x} \in D} \min_{\boldsymbol{\theta} \in \Theta} f(\mathbf{x}, \boldsymbol{\theta})$ , we replace  $\mathbf{x}$  in the original setting by the concatenated input  $(\mathbf{x}, \boldsymbol{\theta})$ , and set

$$d((\mathbf{x}, \boldsymbol{\theta}), (\mathbf{x}', \boldsymbol{\theta}')) = \|\mathbf{x} - \mathbf{x}'\|_2. \quad (68)$$

If we then set  $\epsilon = 0$ , we find that the input  $\mathbf{x}$  experiences no perturbation, whereas  $\boldsymbol{\theta}$  may be perturbed arbitrarily, thereby reducing (7) to  $\max_{\mathbf{x} \in D} \min_{\boldsymbol{\theta} \in \Theta} f(\mathbf{x}, \boldsymbol{\theta})$  as desired.

- For the robust estimation setting, we again use the concatenated input  $(\mathbf{x}, \boldsymbol{\theta})$ . To avoid overloading notation, we let  $d_0(\boldsymbol{\theta}, \boldsymbol{\theta}')$  denote the distance function (applied to  $\boldsymbol{\theta}$  alone) adopted for this case in Section 4. We set

$$d((\mathbf{x}, \boldsymbol{\theta}), (\mathbf{x}', \boldsymbol{\theta}')) = \begin{cases} d_0(\boldsymbol{\theta}, \boldsymbol{\theta}') & \mathbf{x} = \mathbf{x}' \\ \infty & \mathbf{x} \neq \mathbf{x}' \end{cases}. \quad (69)$$

Due to the second case, the input  $\mathbf{x}$  experiences no perturbation, since doing so would violate the distance constraint of  $\epsilon$ . We are then left with  $\mathbf{x} = \mathbf{x}'$  and  $d_0(\boldsymbol{\theta}, \boldsymbol{\theta}') \leq \epsilon$ , as required.

- For the grouped setting  $\max_{G \in \mathcal{G}} \min_{\mathbf{x} \in G} f(\mathbf{x})$ , we adopt the function

$$d(\mathbf{x}, \mathbf{x}') = \mathbf{1}\{\mathbf{x} \text{ and } \mathbf{x}' \text{ are in different groups}\}, \quad (70)$$

and set  $\epsilon = 0$ . Considering the formulation in (7), we find that any two inputs  $\mathbf{x}$  and  $\mathbf{x}'$  yield the same  $\epsilon$ -stable objective function, and hence, reporting a point  $\mathbf{x}$  is equivalent to reporting its group  $G$ . As a result, (7) reduces to the desired formulation  $\max_{G \in \mathcal{G}} \min_{\mathbf{x} \in G} f(\mathbf{x})$ .

The variations of STABLEOPT described in (20)–(26), as well as the corresponding theoretical results outlined in Section 4 follow immediately by substituting the respective choices of  $d(\cdot, \cdot)$  and  $\epsilon$  above into Algorithm 1 and Theorem 1. It should be noted that in the first two examples, the definition of  $\gamma_t$  in (14) is modified to take the maximum over not only  $\mathbf{x}_1, \dots, \mathbf{x}_t$ , but also  $\boldsymbol{\theta}_1, \dots, \boldsymbol{\theta}_t$ .

## D Lake Data Experiment

We consider an application regarding environmental monitoring of inland waters, using a data set containing 2024 in situ measurements of chlorophyll concentration within a vertical transect plane, collected by an autonomous surface vessel in Lake Zürich. This data set was considered in previous

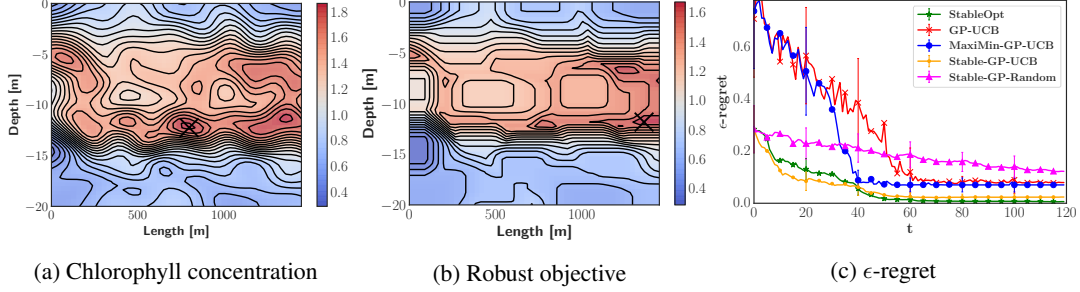


Figure 7: Experiment on the Zürich lake dataset; In the later rounds STABLEOPT is the only method that reports a near-optimal  $\epsilon$ -stable point.

works such as [7, 15] to detect regions of high concentration. In these works, the goal was to locate all regions whose concentration exceeds a pre-defined threshold.

Here we consider a different goal: We seek to locate a region of a given size such that the concentration throughout the region is as high as possible (in the max-min sense). This is of interest in cases where high concentration only becomes relevant when it is spread across a sufficiently wide area. We consider rectangular regions with different pre-specified lengths in each dimension:

$$\Delta_{\epsilon_D, \epsilon_L}(\mathbf{x}) = \{\mathbf{x}' - \mathbf{x} : \mathbf{x}' \in D, |x_D - x'_D| \leq \epsilon_D \cap |x_L - x'_L| \leq \epsilon_L\}, \quad (71)$$

where  $\mathbf{x} = (x_D, x_L)$  and  $\mathbf{x}' = (x'_D, x'_L)$  indicate the depth and length, and we denote the corresponding stability parameters by  $(\epsilon_D, \epsilon_L)$ . This corresponds to  $d(\cdot, \cdot)$  being a weighted  $\ell_\infty$ -norm.

We evaluate each algorithm on a  $50 \times 50$  grid of points, with the corresponding values coming from the GP posterior that was derived using the original data. We use the Matérn-5/2 ARD kernel, setting its hyperparameters by maximizing the likelihood on a second (smaller) available dataset. The parameters  $\epsilon_D$  and  $\epsilon_L$  are set to 1.0 and 100.0, respectively. The stability requirement changes the global maximum and its location, as can be observed in Figure 7. The number of sampling rounds is  $T = 120$ , and each algorithm is initialized with the same 10 random data points and corresponding observations. The performance is averaged over 100 different runs, where every run corresponds to a different random initialization. In this experiment, STABLE-GP-UCB achieves the smallest  $\epsilon$ -regret in the early rounds, while in the later rounds STABLEOPT is the only method that reports a near-optimal  $\epsilon$ -stable point.